

Prediction of residue-residue contacts from protein families using similarity kernels and least squares regularization

Massimo Andreatta¹, Santiago Laplagne¹, Shuai Cheng Li², and Stephen Smale¹

¹Department of Mathematics, City University of Hong Kong, Kowloon, Hong Kong

²Department of Computer Science, City University of Hong Kong, Kowloon, Hong Kong

March 26, 2014

Abstract

One of the most challenging and long-standing problems in computational biology is the prediction of three-dimensional protein structure from amino acid sequence. A promising approach to infer spatial proximity between residues is the study of evolutionary covariance from multiple sequence alignments, especially in light of recent algorithmic improvements and the fast growing size of sequence databases. In this paper, we present a simple, fast and accurate algorithm for the prediction of residue-residue contacts based on regularized least squares. The basic assumption is that spatially proximal residues in a protein coevolve to maintain the physicochemical complementarity of the amino acids involved in the contact. Our regularized inversion of the sample covariance matrix allows the computation of partial correlations between pairs of residues, thereby removing the effect of spurious transitive correlations. The method also accounts for low number of observations by means of a regularization parameter that depends on the effective number of sequences in the alignment. When tested on a set of protein families from Pfam, we found the RLS algorithm to have performance comparable to state-of-the-art methods for contact prediction, while at the same time being faster and conceptually simpler.

The source code and data sets are available at <http://cms.dm.uba.ar/Members/slaplagn/software>

1 Introduction

A major problem in computational biology is the prediction of the 3D structure of a protein from its amino acid sequence. Anfinsen’s dogma suggests that, in principle, the amino acid sequence contains enough information to determine the full three-dimensional structure [1]. However, a few decades on, the mechanisms of protein folding are still not satisfactorily explained [6]. In particular, the space of possible spatial configurations given a certain amino acid 1D sequence is immense (the “Levinthal paradox”), yet an unfolded polypeptide chain is driven to its native 3D structure in a finite time, typically milliseconds to seconds, upon shifting to folding conditions [19].

Such enormous search space poses important challenges to the development of *ab initio* methods for structure prediction. Therefore, it is essential to exploit different kinds of information that can help reduce the degrees of freedom in the configurational search space. A powerful way of inferring distance constraints is the prediction of residue-residue contacts from multiple sequence alignments (MSA). The underlying assumption is that contacting residues coevolve to maintain the physicochemical complementarity of the amino acids involved in the contact. That is, if a mutation occurs in one of the contacting residues, the other one is also likely to mutate, lest the fold of the protein may be disrupted. Methods based on residue coevolution aim at inferring spatial proximity between residues (contacts) from such signals of correlated mutations (Figure 1).

Thanks to the recent exponential growth in sequence data collected in databases such as Pfam [18], algorithms for the prediction of contacting residues from MSA have enjoyed increasing attention. Different kinds of approaches have been recently applied for contact prediction, from mutual information (MI) between pairs of positions [4, 7, 22], to Bayesian network models [3], direct-coupling analysis [2, 17, 15] and

sparse inverse covariance matrix estimation [12]. See also [16] and [5] for recent reviews. In particular, the more sophisticated and successful methods attempt to disentangle direct and indirect correlations, that is the artifactual correlations emerging from transitive effects of covariance analysis [14, 23]. Morcos et al. [17] and Marks et al. [15] tackle this problem using a maximum-entropy approach, whereas Jones et al. [12] estimate partial correlations by inverting the covariance matrix. A very recent pseudo-likelihood method based on 21-state Potts models [9] was shown to outperform other approaches for direct-coupling analysis. Kamisetty et al. [13] systematically analyzed the conditions under which predicted contacts are likely to be useful for structure prediction, and found several hundred families that meet their criteria.

Here, we propose a new approach for computing direct correlations that employs regularized least squares (RLS) regression to invert a sample covariance matrix S . We compute the regularized inverse by the formula

$$\Theta = (S^2 + \eta \text{Id})^{-1}S, \quad (1)$$

with fixed $\eta > 0$. It proves to be a very simple, direct and fast approach, and requires no assumption on probabilities distributions or sparsity in the correlations.

The RLS algorithm described in this paper was applied to three different sets of protein families, and we compared its performance to state-of-the-art methods for contact prediction. The RLS method achieves precision rates superior to PSICOV [12] and comparable to plmDCA [9] but it is considerably faster than either.

2 Approach

2.1 The covariance matrix

Let \mathcal{A} be the set of 20 amino acids plus the gap symbol $-$ and $\mathcal{P} = \{p^m = (p_1^m, \dots, p_L^m)\}_{m=1, \dots, M}$ a given Pfam family of M aligned protein sequences, possibly with gaps, where L denotes the length of the protein domains. On this set of proteins, the covariance between any pair of columns (i, j) for the amino acids pair (a, b) is given by

$$S_{ij}^0(a, b) = f_{ij}(a, b) - f_i(a)f_j(b)$$

where the corrected frequencies are calculated as

$$f_i(a) = \frac{1}{\lambda + M_{\text{eff}}} \left(\frac{\lambda}{21} + \sum_p w(p) \delta(a, p_i) \right) \quad (2)$$

$$f_{ij}(a, b) = \frac{1}{\lambda + M_{\text{eff}}} \left(\frac{\lambda}{21^2} + \sum_p w(p) \delta(a, p_i) \delta(b, p_j) \right)$$

The delta kernel takes value $\delta(a, b) = 1$ if $a = b$ and $\delta(a, b) = 0$ otherwise. $w(p)$ is the weight of protein p and $M_{\text{eff}} = \sum_p w(p)$ (see section 3.1 for details on sequence weighting).

The parameter λ is the so-called pseudocount, a regularization parameter that accounts for non-observed pairs. We note that the same, or similar, constructions for the corrected amino acid frequencies have been proposed previously by other authors [9, 12, 17].

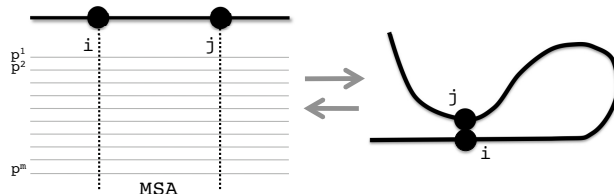


Figure 1: Illustration of a residue-residue contact. The contact imposes a constraint on the evolution of residues i and j . Vice versa, coevolution of i and j can be used to infer their physical proximity.

2.1.1 Modified covariance matrix

We set $S_{ii}^0(a, b) = 0$ for $a \neq b$, and call S this new matrix. This modification also appears in the code of PSICOV [12] although it is not stated in their paper. By setting those values to 0, the resulting matrix contains in general negative eigenvalues (see Figures (2b) and (2d)) and hence is not anymore semi-definite positive, but it is still symmetric. We do not fully understand this step, but it is noteworthy that Equation 1 still makes sense for any $\eta > 0$.

In general, working with S instead of S^0 gives better results in our experiments. See Table S1 for the effect of this step on predictive performance.

2.2 Regularized inverse – the key algorithm

As we mentioned in the Introduction, the covariance between our random variables does not distinguish between direct and indirect correlations. To overcome this problem, a technique used by statisticians is to compute the so-called partial correlations, which can be obtained from the inverse of the covariance matrix using its associated correlation matrix.

Since the covariance matrix is usually singular or ill conditioned, regularization techniques must be used to compute a regularized inverse Θ . We achieve this by solving the following optimization problem

$$\Theta = \underset{X \in \mathbb{R}^{20L \times 20L}}{\operatorname{argmin}} \|SX - \operatorname{Id}\|_2^2 + \eta \|X\|_2^2, \quad (3)$$

where $\|\cdot\|_2$ denotes the Frobenius norm, and η is a regularization parameter to be determined. Observe that the first term is minimized by the inverse of S when it exists.

The problem has a unique solution for any $\eta > 0$ as we see in the next proposition.

Proposition 1. *For a symmetric matrix $S \in \mathbb{R}^{n \times n}$ and a regularization parameter $\eta > 0$, the optimization problem (3) has a unique solution, which is also symmetric and given by equation 1. When S is semidefinite positive, then the solution also is.*

Proof. Since the norms involved are coordinate norms, the problem can be decoupled into independent problems for each column of X :

$$\Theta^{(i)} = \underset{x \in \mathbb{R}^{n \times 1}}{\operatorname{argmin}} \|S^t x - e^{(i)}\|_2^2 + \eta \|x\|_2^2,$$

where $\Theta^{(i)}$ is the i -th column of Θ and $e^{(i)}$ is the i -th column of the identity matrix.

This is a well studied problem known as regularized least squares (also called Tikhonov regularization or Ridge regression in different areas, see [21] and [11]). The unique solution is $\Theta^{(i)} = (S^t S + \eta \operatorname{Id})^{-1} S^t e^{(i)}$.

Hence, the solution to our matrix problem is $\Theta = (S^t S + \eta \operatorname{Id})^{-1} S^t$. Since we are assuming S symmetric, we get

$$\Theta = (S^2 + \eta \operatorname{Id})^{-1} S.$$

The matrix S is diagonalizable with all of its eigenvalues real. The eigenvalues of S are transformed by the same formula defining Θ . If λ_k , $1 \leq k \leq 20L$, are the eigenvalues of S then the eigenvalues of Θ will be

$$\gamma_k = f(\lambda_k) = \frac{\lambda_k}{\lambda_k^2 + \eta}$$

This function is well defined for all $\lambda \in \mathbb{R}$ when η is positive, which proves that the matrix $S^2 + \eta \operatorname{Id}$ is invertible. The resulting matrix Θ is symmetric by standard matrix theory. Finally, f preserves the sign of the eigenvalue and hence Θ will be a semidefinite positive matrix whenever S is. \square

Remark 1. Note that Θ can be computed by solving the linear system $(S^2 + \eta \operatorname{Id})\Theta = S$, which is faster and more accurate than inverting the matrix $S^2 + \eta \operatorname{Id}$.

For a better understanding of our regularization formula, we study the function f in more detail. The derivative of f is $f'(\lambda) = \frac{-\lambda^2 + \eta}{(\lambda^2 + \eta)^2}$. Hence f is increasing for $|\lambda| < \sqrt{\eta}$ and decreasing for $|\lambda| > \sqrt{\eta}$, with maximum value at $\lambda = \sqrt{\eta}$ and minimum value at $\lambda = -\sqrt{\eta}$. We show in Figure (2a) the plot of this function for $\eta = \eta'/M_{\text{eff}} = 1000/3912$ (see Section 3.2 for the choice of η).

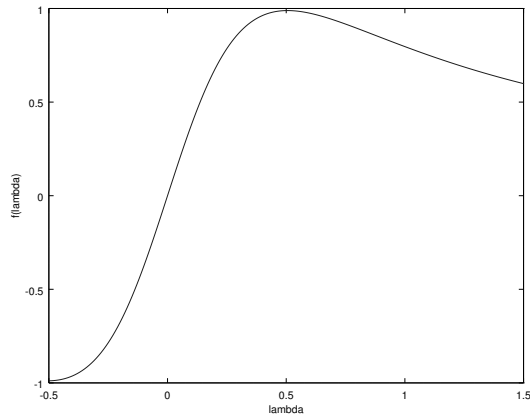
As mentioned in the proof of Proposition 1, the function is smooth at 0, so using this regularization formula we deal in a simple way with the conditioning problem of inverting the covariance matrix.

2.3 Aggregation

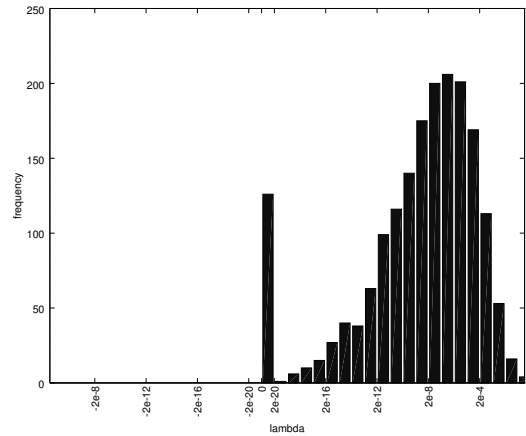
The matrix Θ obtained is a $20L \times 20L$ matrix. Its entries are estimates of the partial correlation between pairs of columns (i, j) for *all* pairs of amino acids (a, b) . Since our goal is to detect relations between pairs of columns in the alignment, we compute a coupling score aggregating the values of Θ using the l_1 -norm on the 20×20 sub-matrices, as in [12]. That is,

$$P(i, j) = \sum_{1 \leq a, b \leq 20} |\Theta_{ij}(a, b)|.$$

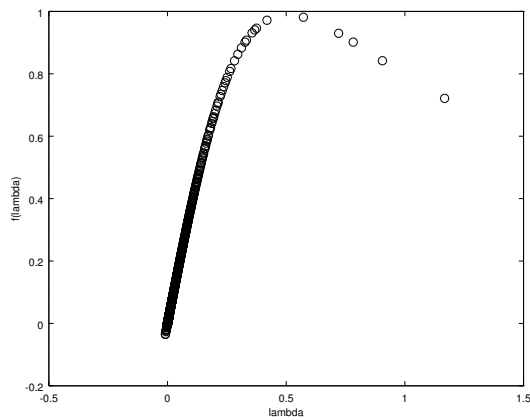
The l_2 -norm for aggregation showed poorer performance than the l_1 -norm above. Finally, following [7] and



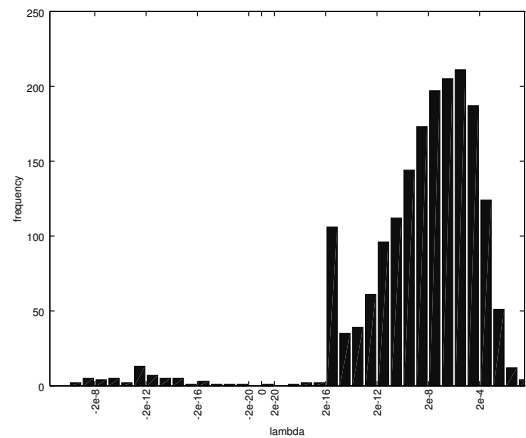
(a) Function $f(\lambda) = \frac{\lambda}{\lambda^2 + \eta}$, $\eta = \eta'/M_{\text{eff}} = 1000/3912$



(b) Distribution of eigenvalues of the covariance matrix S_0



(c) Relation between the eigenvalues of the modified covariance matrix S and its regularized inverse Θ



(d) Distribution of eigenvalues of the modified covariance matrix S

Figure 2: Distribution of eigenvalues of the covariance matrix and its regularized inverse for PFAM family PF00028.

[12] we define a corrected score $P_{\text{APC}}(i, j) = P(i, j) - \frac{P(\cdot, j)P(i, \cdot)}{P(\cdot, \cdot)}$, where \cdot stands for the average over all positions.

The prediction of contacts between pairs of residues can now be obtained by ranking the $P_{\text{APC}}(i, j)$, where higher scores identify more likely residue-residue contacts.

3 Method details

In this section we give more details on the actual implementation of the algorithm described above.

3.1 Sequence weighting

Families from the Pfam database contain some degree of redundancy. A common strategy to overcome this problem is sequence weighting, which weighs down groups of similar sequences and assigns higher weights to isolated sequences.

We first define a similarity measure between proteins, following [20]. We start from the BLOSUM90 frequency substitution matrix $B_{90}(a, b)$ defined in [10] and call $\hat{B}_{90}(a, b)$ for a pair of amino acids (a, b) the normalized matrix

$$\hat{B}_{90}(a, b) = \frac{B_{90}(a, b)}{\sqrt{B_{90}(a, a)B_{90}(b, b)}}$$

We then proceed to construct a similarity kernel between pairs of proteins

$$K^3(p, q) = \sum_{k=1}^{10} \left(\sum_{i=1}^{L-k+1} K^2((p_i \dots p_{i+k-1}), (q_i \dots q_{i+k-1})) \right)$$

where

$$K^2((p_i \dots p_{i+k-1}), (q_i \dots q_{i+k-1})) = \prod_{j=1}^k \hat{B}_{90}(p_{i+j-1}, q_{i+j-1}),$$

for $p, q \in \mathcal{P}$, $1 \leq k \leq L$ and $1 \leq i \leq L - k + 1$;

The normalized version of K^3 is obtained using

$$\hat{K}^3(p, q) = \frac{K^3(p, q)}{\sqrt{K^3(p, p)K^3(q, q)}}.$$

Note that, since Pfam families consist of pre-aligned sequences, our K^3 kernel definition differs slightly from [20] as it only compares aligned amino acid k -mers. Also, we limit the k -mers considered in the construction of K^3 to lengths smaller or equal to 10. This implies a substantial improvement in computation time, with no significant loss in predictive power.

We fix a threshold θ (in this paper, $\theta = 0.7$) and for any protein $p \in \mathcal{P}$ we define the equilibrium measure

$$\pi(p) = \sum_{\substack{q \in \mathcal{P} \\ \hat{K}^3(p, q) > (1-\theta)}} \hat{K}^3(p, q).$$

The weight of a protein p is then defined as the reciprocal of the equilibrium measure $w(p) = (\pi(p))^{-1}$, and the effective number of sequences in the alignment is $M_{\text{eff}} = \sum_p w(p)$. The kernel $\hat{K}^3(p, q)$ is a measure of similarity between pairs of proteins, and for a given protein p the quantity $\pi(p)$ effectively counts the number of sequences with similarity larger than a threshold $1 - \theta$, thereby weighing down sequences that are over-represented in the data set.

Hamming distance weighting As a term of comparison, we also applied a more traditional sequence weighting scheme based on the hamming distance between pairs of sequences. For each sequence p , we count the number of other sequences in the alignment that share more than $\theta\%$ sequence identity with p

$$m^p = |\{b \in \{1, \dots, M\} : \%id(p, b) > \theta\}|$$

and then assign a weight $w(p) = 1/m^p$ to sequence p .

This approach was used previously by several authors such as [17], [12] and [9], but we note that these authors use different values for the threshold θ (respectively 0.8, 0.62 and 0.9). In this paper we choose $\theta = 0.62$. See See Tables S2-S3 for the optimization of the two weighting schemes with respect to the regularization parameter η' , and Table S4 for a comparison of their performance.

3.2 Regularization parameter

The matrix inversion in Equation 1 contains a regularization parameter η . We observed that families containing few sequences, where the number of sequences M is comparable in size to the number of random variables ($20L$) require a larger regularization parameter compared to bigger families ($M \gg 20L$). We use then a regularization parameter of the form $\eta = \eta'/M_{\text{eff}}$, where M_{eff} is the effective number of sequences defined above.

We tried different values of η' over the 15 families from [15], and observed that in general roughly the same η' appears to be optimal across families with different M_{eff} . Thus the normalization $\eta = \eta'/M_{\text{eff}}$ appears appropriate.

In Figure (2c) we show how the actual eigenvalues of the modified covariance matrix corresponding to PFAM family PF00028 are transformed when computing the regularized inverse.

3.3 Pseudocounts

The pseudocounts parameter λ in Equation 2 accounts for non-observed pairs of amino acids. Following [17], we set $\lambda = 44$. However, we observed that the performance gain is small compared to setting $\lambda = 0$ (see Table S5). In fact, pseudocounts have a similar regularizing effect to the parameter η' described in the previous section, and probably for this reason the contribution of λ is minimal.

4 Results and Conclusion

The method and estimation of parameters described above were first applied to the 15 families studied in Marks et al. [15]. Performance was estimated in terms of the fraction of correct predicted contacts among the $L/5$, $L/3$, $L/2$ and L pairs with highest P_{APC} score, where L is the length of the alignment. We considered as a true contact a pair of amino acids with beta-carbons ($C\beta$) with distance $< 8 \text{ \AA}$ and at least

Table 1: Positive predictive value for partial correlation scores in the set of 15 families from [15], measured on $C\beta$ carbons

PFAM	PDB	L	M	M_{eff}	top $L/5$			top $L/3$			top $L/2$			top L		
					RLS	PSICOV	DCA	RLS	PSICOV	DCA	RLS	PSICOV	DCA	RLS	PSICOV	DCA
PF00001	1hxx	257	23711	3610	0.608	0.549	0.417	0.565	0.494	0.333	0.516	0.453	0.281	0.374	0.300	0.222
PF00013	1wvn	56	5298	1710	0.909	0.818	0.909	0.889	0.778	0.944	0.857	0.643	0.926	0.679	0.518	0.655
PF00014	5pti	48	1743	1019	0.889	0.889	1.000	0.625	0.750	0.750	0.750	0.750	0.750	0.625	0.542	0.604
PF00018	2hda	45	3610	1529	0.889	0.889	0.889	0.933	0.933	0.933	0.909	0.864	0.818	0.667	0.622	0.667
PF00028	2o72	91	8828	3912	0.944	0.944	0.823	0.933	0.933	0.862	0.889	0.889	0.909	0.802	0.791	0.809
PF00059	2it6	107	4067	1949	0.810	0.810	0.850	0.771	0.743	0.765	0.774	0.736	0.726	0.598	0.561	0.628
PF00071	5p21	161	8395	1868	0.844	0.813	0.774	0.811	0.755	0.811	0.763	0.725	0.798	0.652	0.627	0.604
PF00072	1e6k	108	45821	24642	0.810	0.857	0.857	0.778	0.861	0.857	0.759	0.815	0.793	0.685	0.694	0.755
PF00075	1f21	126	8131	960	0.760	0.680	0.680	0.738	0.714	0.610	0.714	0.667	0.581	0.579	0.524	0.520
PF00076	1g2e	70	18491	6849	0.786	0.786	0.786	0.870	0.783	0.870	0.857	0.829	0.914	0.757	0.743	0.814
PF00085	1rqm	100	9095	3814	0.800	0.700	0.842	0.758	0.758	0.688	0.740	0.700	0.729	0.650	0.570	0.639
PF00089	3tgi	217	12909	4296	0.977	0.837	0.951	0.847	0.750	0.855	0.796	0.713	0.789	0.724	0.595	0.673
PF00254	1r9h	95	5269	1759	0.895	0.895	0.889	0.807	0.839	0.936	0.851	0.745	0.891	0.674	0.579	0.667
PF00307	1bkr	107	2751	873	0.714	0.333	0.700	0.629	0.229	0.697	0.547	0.264	0.500	0.449	0.252	0.455
PF00486	1odd	74	13702	5452	0.786	0.786	0.714	0.708	0.583	0.667	0.649	0.541	0.583	0.527	0.419	0.521
Average					0.828	0.772	0.805	0.777	0.727	0.772	0.758	0.689	0.732	0.629	0.556	0.615

5 residues apart along the length of the protein. We find that on these 15 families the optimal value for the regularization parameter is around $\eta' = 1000$ (see Table S2).

Table 1 compares the performance of the RLS algorithm with PSICOV version 1.11 [12] and the plmDCA method [9]. We observe that on this set our method outperforms both PSICOV and DCA on the majority of families. Additionally, in Table S6 in shown the positive predictive value of the methods with respect to short range ($5 \leq i - j \leq 11$), medium range ($12 \leq i - j \leq 23$) and long range (> 23) interactions for the prediction of the top $L/5$ contacts.

Next, we applied the three methods using the same parameters on an additional set of families from [9]. This set partially overlapped with the families from [15] studied in Table 1, and after removing the duplicates we are left with a set of 22 families. Table 2 shows the positive predictive value of the RLS algorithm compared to PSICOV and plmDCA. On this set plmDCA obtains the highest average performance on three out of four ranking categories. However, note that plmDCA was optimized on this set of families, so there may be a bias in favor of this method.

Finally, we constructed an independent set of 10 families, selected randomly from Pfam with the only condition of containing at least 1,000 unique sequences. This set had not been used in the optimization of the algorithms, therefore constitutes a fair ground for comparison. The results (see Table 3) show that RLS outperforms the other two methods in the $L/5$ and $L/3$ subsets, whereas DCA obtains highest average performance for the prediction of the top $L/2$ and L contacts.

A comparison of the running times of the two best algorithms (RLS and DCA) shows that RLS is at least one order of magnitude faster than DCA (Table 4). Note that we used the latest fast version of plmDCA [8], termed ‘‘asymmetric plmDCA’’, which improves considerably on previous pseudolikelihood methods in terms of speed. Our fast regularized inversion of the covariance matrix allows contact prediction on

Table 2: Positive predictive value for partial correlation scores in a set of 22 families from [9], measured on $C\beta$ carbons

PFAM	PDB	L	M	M_{eff}	top $L/5$			top $L/3$			top $L/2$			top L		
					RLS	PSICOV	DCA	RLS	PSICOV	DCA	RLS	PSICOV	DCA	RLS	PSICOV	DCA
PF00006	2r9v	213	13515	161	0.429	0.310	0.634	0.366	0.282	0.638	0.330	0.255	0.625	0.239	0.202	0.450
PF00011	2bol	100	6600	2622	0.800	0.750	0.875	0.788	0.576	0.815	0.660	0.520	0.756	0.530	0.450	0.578
PF00017	1o47	75	4911	1361	0.800	0.733	0.733	0.760	0.680	0.680	0.676	0.568	0.622	0.493	0.440	0.547
PF00025	1fzq	172	4384	659	0.647	0.559	0.500	0.544	0.509	0.518	0.454	0.407	0.482	0.326	0.308	0.324
PF00026	3er5	317	4326	1445	0.810	0.762	0.800	0.752	0.667	0.733	0.753	0.658	0.717	0.596	0.489	0.586
PF00027	3fhi	89	16544	8545	1.000	1.000	1.000	1.000	0.966	1.000	0.977	0.909	1.000	0.843	0.809	0.888
PF00032	1zrt	80	30643	702	0.750	0.688	0.500	0.615	0.615	0.462	0.500	0.450	0.400	0.263	0.263	0.238
PF00035	1o0w	64	4254	1958	0.917	0.917	1.000	0.952	0.857	0.952	0.906	0.688	0.903	0.609	0.531	0.714
PF00041	1bqu	82	33103	11568	0.688	0.938	0.813	0.741	0.704	0.731	0.659	0.610	0.650	0.585	0.524	0.588
PF00043	6gsu	93	8822	2653	0.556	0.500	0.563	0.452	0.419	0.500	0.348	0.370	0.429	0.258	0.237	0.321
PF00044	1crw	144	8047	838	0.893	0.857	0.929	0.813	0.833	0.870	0.722	0.736	0.814	0.618	0.611	0.700
PF00046	2vi6	57	10117	1376	0.455	0.636	0.500	0.526	0.474	0.471	0.429	0.393	0.385	0.281	0.263	0.264
PF00056	1a5z	137	5673	813	0.852	0.704	0.926	0.844	0.578	0.867	0.765	0.529	0.821	0.569	0.416	0.615
PF00073	2r06	170	11796	136	0.353	0.206	0.094	0.250	0.125	0.111	0.224	0.094	0.111	0.165	0.112	0.117
PF00081	3bfr	76	4017	619	0.600	0.467	0.429	0.520	0.480	0.458	0.421	0.368	0.514	0.263	0.290	0.351
PF00084	1elv	53	13038	5457	0.700	0.600	0.667	0.706	0.471	0.625	0.692	0.577	0.625	0.472	0.491	0.521
PF00091	2r75	215	10854	321	0.442	0.488	0.706	0.352	0.380	0.614	0.299	0.355	0.547	0.265	0.261	0.407
PF00092	1atz	177	7070	1799	0.714	0.771	0.758	0.695	0.780	0.582	0.716	0.727	0.566	0.588	0.593	0.530
PF00105	1gdc	64	3595	663	0.667	0.667	0.833	0.619	0.619	0.619	0.500	0.500	0.581	0.344	0.375	0.444
PF00107	1a71	128	24755	7021	0.880	0.840	0.913	0.833	0.810	0.790	0.750	0.781	0.776	0.633	0.602	0.690
PF00108	3goa	261	9701	1680	0.750	0.731	0.778	0.713	0.644	0.733	0.685	0.685	0.735	0.605	0.563	0.678
PF00111	1a70	74	10559	2848	0.643	0.571	0.615	0.542	0.458	0.409	0.432	0.405	0.394	0.405	0.378	0.303
Average					0.697	0.668	0.708	0.654	0.588	0.644	0.586	0.527	0.612	0.452	0.418	0.493

Table 3: Positive predictive value for partial correlation scores in a new set of 10 families, measured on $C\beta$ carbons

PFAM	PDB	L	M	M_{eff}	top $L/5$			top $L/3$			top $L/2$			top L		
					RLS	PSICOV	DCA	RLS	PSICOV	DCA	RLS	PSICOV	DCA	RLS	PSICOV	DCA
PF00240	4k7s	69	5382	1809	0.923	0.846	0.846	0.870	0.783	0.905	0.765	0.677	0.875	0.580	0.449	0.600
PF00390	1qr6	182	3865	182	0.583	0.583	0.314	0.467	0.450	0.373	0.396	0.330	0.292	0.247	0.242	0.225
PF00482	2vmb	124	8131	3673	0.833	0.583	0.857	0.829	0.537	0.800	0.742	0.403	0.808	0.460	0.282	0.590
PF00793	3stc	256	4878	506	0.628	0.294	0.556	0.494	0.294	0.513	0.414	0.234	0.474	0.289	0.184	0.411
PF01026	1xwy	244	5507	1907	0.833	0.771	0.792	0.815	0.741	0.775	0.746	0.664	0.758	0.648	0.562	0.679
PF01791	3myp	233	3865	673	0.261	0.304	0.273	0.286	0.286	0.288	0.250	0.267	0.255	0.206	0.197	0.223
PF01807	2au3	92	2773	837	0.778	0.833	0.824	0.800	0.767	0.862	0.826	0.848	0.886	0.707	0.707	0.753
PF03484	1b7y	62	2669	1265	1.000	0.750	1.000	0.950	0.850	0.900	0.903	0.774	0.933	0.726	0.629	0.754
PF12704	3ftj	231	14338	7373	0.891	0.717	0.919	0.844	0.546	0.853	0.800	0.452	0.804	0.597	0.286	0.643
PF13305	3on2	80	1583	964	0.500	0.438	0.400	0.308	0.269	0.360	0.225	0.200	0.263	0.163	0.163	0.145
Average					0.723	0.612	0.678	0.666	0.552	0.663	0.607	0.485	0.635	0.462	0.370	0.502

Table 4: Running times for the RLS and plmDCA (asymmetric) algorithms, in seconds. Both algorithms were run on the same computer, using a fixed number of 4 processors.

Pfam	Length	RLS	plmDCA
PF00001	257	21.9	2429.5
PF00013	56	0.3	25.8
PF00014	48	0.2	9.1
PF00018	45	0.2	11.9
PF00028	91	1.2	103.5
PF00059	107	1.5	73.2
PF00071	161	5.0	319.0
PF00072	108	5.0	686.0
PF00075	126	2.7	177.9
PF00076	70	1.0	108.1
PF00085	100	1.6	128.7
PF00089	217	11.5	1029.3
PF00254	95	1.2	69.8
PF00307	107	1.4	49.0
PF00486	74	0.9	104.6

hundreds of amino acids-long domains in a matter of seconds, practically removing the limitations on the length of proteins that can be analyzed. In fact, the slowest step in the predictions is sequence weighting (not accounted in Table 4 for either method), in particular the K^3 -based weighting can be slow for very large families, but we showed that a simpler and faster weighting strategy does not affect too dramatically the performance (Table S4).

In general, we observed that the performance depends on the effective number of sequences M_{eff} in the alignment. For instance, families PF00390 or PF00793 are composed of several thousand sequences, but they contain much redundancy, which brings down M_{eff} to a few hundred units. Roughly, it appears that at least 1000 non-redundant sequences ($M_{\text{eff}} > 1000$) are necessary to achieve a reasonable precision for contact prediction. This is in agreement with previous estimates [15, 13] which place this number at about $5L$, where L is the length of the alignment.

In conclusion, we demonstrated how our simple regularization scheme for covariance matrix inversion allows the fast and accurate prediction of residue-residue contacts. Currently, a major restriction to this kind of approach is the fairly high number of non-redundant sequences required to infer coevolution from a multiple sequence alignment, limiting the application to a relatively small subset of Pfam. However, as the number of protein sequences deposited in public databases increases, we expect a larger number of protein families to become accessible to our analysis, as well as improved performance on those that are already accessible.

Acknowledgement

This work received funding from City University of Hong Kong grants RGC #9380050 and #9041544. Work by S.L. was partially supported by Ministerio de Ciencia, Tecnología e Innovación Productiva, Argentina.

References

- [1] Christian B Anfinsen. Principles that govern the folding of protein chains. *Science*, 181(4096):223–230, 1973.
- [2] Sivaraman Balakrishnan, Hetunandan Kamisetty, Jaime G Carbonell, Su-In Lee, and Christopher James Langmead. Learning generative models for protein fold families. *Proteins: Structure, Function, and Bioinformatics*, 79(4):1061–1078, 2011.
- [3] Lukas Burger and Erik van Nimwegen. Disentangling direct from indirect co-evolution of residues in protein alignments. *PLoS computational biology*, 6(1):e1000633, 2010.

- [4] Cristina Marino Buslje, Javier Santos, Jose Maria Delfino, and Morten Nielsen. Correction for phylogeny, small number of observations and data redundancy improves the identification of coevolving amino acid pairs using mutual information. *Bioinformatics*, 25(9):1125–1131, 2009.
- [5] David de Juan, Florencio Pazos, and Alfonso Valencia. Emerging methods in protein co-evolution. *Nature Reviews Genetics*, 14(4):249–261, 2013.
- [6] Ken A Dill and Justin L MacCallum. The protein-folding problem, 50 years on. *Science*, 338(6110):1042–1046, 2012.
- [7] Stanley D Dunn, Lindi M Wahl, and Gregory B Gloor. Mutual information without the influence of phylogeny or entropy dramatically improves residue contact prediction. *Bioinformatics*, 24(3):333–340, 2008.
- [8] Magnus Ekeberg, Tuomo Hartonen, and Erik Aurell. Fast pseudolikelihood maximization for direct-coupling analysis of protein structure from many homologous amino-acid sequences. *arXiv preprint arXiv:1401.4832*, 2014.
- [9] Magnus Ekeberg, Cecilia Lövkvist, Yueheng Lan, Martin Weigt, and Erik Aurell. Improved contact prediction in proteins: using pseudolikelihoods to infer Potts models. *Physical Review E*, 87(1):012707, 2013.
- [10] Steven Henikoff and Jorja G Henikoff. Amino acid substitution matrices from protein blocks. *Proceedings of the National Academy of Sciences*, 89(22):10915–10919, 1992.
- [11] Arthur E Hoerl. Application of ridge analysis to regression problems. *Chemical Engineering Progress*, 58(3):54–59, 1962.
- [12] David T Jones, Daniel WA Buchan, Domenico Cozzetto, and Massimiliano Pontil. PSICOV: precise structural contact prediction using sparse inverse covariance estimation on large multiple sequence alignments. *Bioinformatics*, 28(2):184–190, 2012.
- [13] Hetunandan Kamisetty, Sergey Ovchinnikov, and David Baker. Assessing the utility of coevolution-based residue–residue contact predictions in a sequence and structure-rich era. *Proceedings of the National Academy of Sciences*, 110(39):15674–15679, 2013.
- [14] Alan S Lapedes, Bertrand G Giraud, LonChang Liu, and Gary D Stormo. Correlated mutations in models of protein sequences: phylogenetic and structural effects. *Lecture Notes-Monograph Series*, pp. 236–256, 1999.
- [15] Debora S Marks, Lucy J Colwell, Robert Sheridan, Thomas A Hopf, Andrea Pagnani, Riccardo Zecchina, and Chris Sander. Protein 3D structure computed from evolutionary sequence variation. *PLoS One*, 6(12):e28766, 2011.
- [16] Debora S Marks, Thomas A Hopf, and Chris Sander. Protein structure prediction from sequence variation. *Nature biotechnology*, 30(11):1072–1080, 2012.
- [17] Faruck Morcos, Andrea Pagnani, Bryan Lunt, Arianna Bertolino, Debora S Marks, Chris Sander, Riccardo Zecchina, José N Onuchic, Terence Hwa, and Martin Weigt. Direct-coupling analysis of residue coevolution captures native contacts across many protein families. *Proceedings of the National Academy of Sciences*, 108(49):E1293–E1301, 2011.
- [18] Marco Punta, Penny C Coggill, Ruth Y Eberhardt, Jaina Mistry, John Tate, Chris Boursnell, Ningze Pang, Kristoffer Forslund, Goran Ceric, Jody Clements, et al. The Pfam protein families database. *Nucleic acids research*, 40(D1):D290–D301, 2012.
- [19] George D Rose, Patrick J Fleming, Jayanth R Banavar, and Amos Maritan. A backbone-based theory of protein folding. *Proceedings of the National Academy of Sciences*, 103(45):16623–16633, 2006.

- [20] Wen-Jun Shen, Hau-San Wong, Quan-Wu Xiao, Xin Guo, and Stephen Smale. Introduction to the peptide binding problem of computational immunology: New results. *Foundations of Computational Mathematics*, pp. 1–34, 2013.
- [21] Andrey Nikolayevich Tikhonov. On the stability of inverse problems. *Dokl. Akad. Nauk SSSR*, 39(5):195–198, 1943.
- [22] Zhiyong Wang and Jinbo Xu. Predicting protein contact map using evolutionary and physical constraints by integer programming. *Bioinformatics*, 29(13):i266–i273, 2013.
- [23] Martin Weigt, Robert A White, Hendrik Szurmant, James A Hoch, and Terence Hwa. Identification of direct residue contacts in protein–protein interaction by message passing. *Proceedings of the National Academy of Sciences*, 106(1):67–72, 2009.

Table S1: Positive predictive value of RLS algorithm on 4 different schemes, using $\eta^i=1000$.

FAM	Top L/5				Top L/3				Top L/2				Top L			
	M1 $\lambda=44, S$	M2 $\lambda=0, S$	M3 $\lambda=44, S0$	M4 $\lambda=0, S0$	M1 $\lambda=44, S$	M2 $\lambda=0, S$	M3 $\lambda=44, S0$	M4 $\lambda=0, S0$	M1 $\lambda=44, S$	M2 $\lambda=0, S$	M3 $\lambda=44, S0$	M4 $\lambda=0, S0$	M1 $\lambda=44, S$	M2 $\lambda=0, S$	M3 $\lambda=44, S0$	M4 $\lambda=0, S0$
PF00001	0.608	0.608	0.608	0.588	0.565	0.553	0.541	0.541	0.516	0.523	0.477	0.477	0.374	0.358	0.370	0.354
PF00013	0.909	0.818	0.909	0.818	0.889	0.889	0.889	0.778	0.857	0.821	0.857	0.821	0.679	0.661	0.679	0.625
PF00014	0.889	0.889	0.889	0.889	0.625	0.688	0.688	0.688	0.750	0.750	0.750	0.708	0.625	0.625	0.625	0.604
PF00018	0.889	0.889	0.889	0.889	0.933	0.933	0.933	0.933	0.909	0.818	0.864	0.864	0.667	0.644	0.667	0.667
PF00028	0.944	0.944	0.944	0.944	0.933	0.900	0.900	0.900	0.889	0.889	0.889	0.889	0.802	0.813	0.791	0.791
PF00059	0.810	0.810	0.810	0.810	0.771	0.800	0.800	0.829	0.774	0.774	0.774	0.774	0.598	0.570	0.589	0.579
PF00071	0.844	0.844	0.844	0.844	0.811	0.811	0.811	0.811	0.763	0.763	0.763	0.775	0.652	0.646	0.646	0.640
PF00072	0.810	0.810	0.810	0.810	0.778	0.778	0.778	0.778	0.759	0.759	0.759	0.759	0.685	0.685	0.639	0.639
PF00075	0.760	0.720	0.760	0.760	0.738	0.691	0.762	0.691	0.714	0.698	0.714	0.667	0.579	0.540	0.548	0.524
PF00076	0.786	0.786	0.786	0.786	0.870	0.870	0.870	0.870	0.857	0.857	0.857	0.857	0.757	0.757	0.686	0.686
PF00085	0.800	0.800	0.800	0.800	0.758	0.758	0.758	0.758	0.740	0.740	0.720	0.720	0.650	0.640	0.640	0.640
PF00089	0.977	0.977	0.977	0.977	0.847	0.847	0.875	0.875	0.796	0.796	0.824	0.824	0.724	0.724	0.687	0.673
PF00254	0.895	0.895	0.895	0.895	0.807	0.807	0.774	0.774	0.851	0.830	0.851	0.851	0.674	0.663	0.653	0.684
PF00307	0.714	0.714	0.762	0.762	0.629	0.686	0.657	0.686	0.547	0.623	0.566	0.604	0.449	0.439	0.486	0.467
PF00486	0.786	0.786	0.714	0.714	0.708	0.708	0.708	0.750	0.649	0.649	0.595	0.649	0.527	0.514	0.500	0.473
Average	0.828	0.819	0.826	0.819	0.777	0.781	0.783	0.777	0.758	0.753	0.751	0.749	0.629	0.619	0.614	0.603

M1: pseudocounts $\lambda=44$, covariance matrix S
M2: pseudocounts $\lambda=0$, covariance matrix S
M3: pseudocounts $\lambda=44$, covariance matrix S0
M4: pseudocounts $\lambda=0$, covariance matrix S0

Table S2: Positive predictive value of the RLS algorithm for different value of the regularization parameter η' , using K3 for weighting

FAM	Top L/5					Top L/3					Top L/2					Top L				
	$\eta'=100$	$\eta'=500$	$\eta'=1000$	$\eta'=2000$	$\eta'=5000$	$\eta'=100$	$\eta'=500$	$\eta'=1000$	$\eta'=2000$	$\eta'=5000$	$\eta'=100$	$\eta'=500$	$\eta'=1000$	$\eta'=2000$	$\eta'=5000$	$\eta'=100$	$\eta'=500$	$\eta'=1000$	$\eta'=2000$	$\eta'=5000$
PF00001	0.471	0.569	0.608	0.628	0.647	0.459	0.565	0.565	0.565	0.506	0.422	0.484	0.516	0.500	0.500	0.339	0.374	0.374	0.370	0.346
PF00013	1.000	0.909	0.909	0.909	0.909	0.889	0.889	0.889	0.889	0.889	0.750	0.786	0.857	0.893	0.893	0.571	0.696	0.679	0.679	0.625
PF00014	0.889	0.889	0.889	0.778	0.556	0.750	0.750	0.625	0.625	0.625	0.583	0.708	0.750	0.750	0.750	0.542	0.583	0.625	0.625	0.625
PF00018	0.889	0.889	0.889	0.889	0.889	0.867	0.933	0.933	0.933	0.867	0.773	0.864	0.909	0.864	0.909	0.711	0.667	0.667	0.644	0.644
PF00028	0.944	0.944	0.944	0.889	0.889	0.900	0.933	0.933	0.933	0.933	0.867	0.867	0.889	0.889	0.867	0.758	0.813	0.802	0.802	0.780
PF00059	0.762	0.810	0.810	0.810	0.857	0.771	0.771	0.771	0.771	0.714	0.717	0.755	0.774	0.717	0.679	0.542	0.608	0.598	0.561	0.579
PF00071	0.813	0.844	0.844	0.844	0.844	0.755	0.830	0.811	0.755	0.755	0.775	0.750	0.763	0.775	0.750	0.584	0.652	0.652	0.640	0.590
PF00072	0.810	0.762	0.810	0.857	0.857	0.861	0.778	0.778	0.806	0.833	0.833	0.796	0.759	0.778	0.778	0.685	0.667	0.685	0.713	0.713
PF00075	0.720	0.760	0.760	0.720	0.720	0.643	0.738	0.738	0.738	0.691	0.619	0.698	0.714	0.714	0.683	0.484	0.579	0.579	0.548	0.532
PF00076	0.786	0.786	0.786	0.786	0.786	0.826	0.870	0.870	0.870	0.826	0.829	0.857	0.857	0.857	0.857	0.671	0.729	0.757	0.743	0.729
PF00085	0.850	0.800	0.800	0.800	0.750	0.758	0.758	0.758	0.727	0.697	0.740	0.740	0.740	0.740	0.700	0.630	0.660	0.650	0.620	0.610
PF00089	0.837	0.977	0.977	0.977	0.954	0.778	0.819	0.847	0.861	0.861	0.759	0.796	0.796	0.787	0.778	0.627	0.710	0.724	0.719	0.696
PF00254	0.895	0.895	0.895	0.790	0.790	0.903	0.839	0.807	0.774	0.774	0.894	0.851	0.851	0.809	0.745	0.653	0.653	0.674	0.653	0.621
PF00307	0.762	0.714	0.714	0.667	0.476	0.543	0.629	0.629	0.486	0.457	0.528	0.585	0.547	0.509	0.453	0.411	0.477	0.449	0.421	0.365
PF00486	0.643	0.714	0.786	0.714	0.643	0.625	0.750	0.708	0.750	0.667	0.595	0.676	0.649	0.595	0.595	0.500	0.514	0.527	0.460	0.446
Average	0.805	0.817	0.828	0.804	0.771	0.755	0.790	0.777	0.766	0.740	0.712	0.748	0.758	0.745	0.729	0.581	0.625	0.629	0.613	0.593

Table S3: Positive predictive value of the RLS algorithm for different value of the regularization parameter η' , using Hamming distance at 62% for weighting

FAM	Top L/5					Top L/3					Top L/2					Top L				
	$\eta'=100$	$\eta'=250$	$\eta'=500$	$\eta'=1000$	$\eta'=2000$	$\eta'=100$	$\eta'=250$	$\eta'=500$	$\eta'=1000$	$\eta'=2000$	$\eta'=100$	$\eta'=250$	$\eta'=500$	$\eta'=1000$	$\eta'=2000$	$\eta'=100$	$\eta'=250$	$\eta'=500$	$\eta'=1000$	$\eta'=2000$
PF00001	0.471	0.510	0.569	0.608	0.647	0.435	0.482	0.541	0.577	0.565	0.391	0.461	0.484	0.500	0.484	0.296	0.319	0.346	0.362	0.358
PF00013	0.909	0.909	0.909	0.909	0.909	0.833	0.889	0.889	0.944	0.889	0.750	0.857	0.821	0.857	0.857	0.536	0.625	0.643	0.643	0.607
PF00014	0.889	0.889	0.889	0.889	0.889	0.688	0.750	0.688	0.625	0.625	0.625	0.667	0.708	0.708	0.708	0.521	0.563	0.563	0.542	0.563
PF00018	0.889	0.889	0.889	0.889	0.889	0.867	0.867	0.933	0.933	0.933	0.773	0.864	0.909	0.909	0.909	0.689	0.667	0.667	0.644	0.622
PF00028	0.944	0.944	0.944	0.944	0.889	0.867	0.867	0.900	0.933	0.933	0.867	0.867	0.889	0.867	0.867	0.758	0.780	0.813	0.813	0.780
PF00059	0.810	0.810	0.857	0.857	0.810	0.800	0.771	0.771	0.771	0.714	0.736	0.774	0.774	0.717	0.698	0.542	0.570	0.617	0.551	0.523
PF00071	0.813	0.844	0.875	0.875	0.875	0.755	0.793	0.811	0.830	0.811	0.738	0.800	0.788	0.775	0.750	0.571	0.627	0.646	0.658	0.646
PF00072	0.810	0.762	0.762	0.810	0.857	0.861	0.806	0.778	0.806	0.833	0.815	0.815	0.796	0.796	0.815	0.694	0.713	0.713	0.722	0.732
PF00075	0.680	0.680	0.720	0.720	0.720	0.548	0.619	0.643	0.667	0.667	0.540	0.587	0.619	0.651	0.667	0.437	0.492	0.548	0.540	0.540
PF00076	0.786	0.786	0.786	0.786	0.857	0.870	0.870	0.870	0.826	0.826	0.829	0.829	0.857	0.857	0.829	0.729	0.757	0.743	0.743	0.771
PF00085	0.800	0.800	0.800	0.800	0.800	0.788	0.818	0.727	0.727	0.697	0.740	0.700	0.720	0.740	0.720	0.620	0.670	0.680	0.660	0.620
PF00089	0.837	0.907	0.954	0.977	0.954	0.764	0.875	0.833	0.819	0.833	0.713	0.796	0.815	0.787	0.778	0.595	0.664	0.687	0.696	0.668
PF00254	0.842	0.895	0.895	0.842	0.790	0.871	0.807	0.807	0.807	0.807	0.872	0.851	0.809	0.766	0.702	0.632	0.632	0.632	0.611	0.621
PF00307	0.571	0.667	0.714	0.714	0.571	0.571	0.600	0.571	0.543	0.543	0.528	0.509	0.528	0.491	0.453	0.421	0.430	0.430	0.439	0.411
PF00486	0.714	0.714	0.714	0.714	0.786	0.625	0.625	0.708	0.667	0.667	0.595	0.676	0.622	0.568	0.622	0.541	0.527	0.554	0.500	0.487
Average	0.784	0.800	0.818	0.822	0.801	0.743	0.763	0.765	0.770	0.756	0.701	0.737	0.743	0.733	0.724	0.572	0.602	0.619	0.608	0.597

Table S4: Positive predictive value using K3 and Hamming distance for sequence weighting, using optimal η' from tables S2 and S3

FAM	Top L/5		Top L/3		Top L/2		Top L	
	K3 $\eta'=1000$	Ham62 $\eta'=500$	K3 $\eta'=1000$	Ham62 $\eta'=500$	K3 $\eta'=1000$	Ham62 $\eta'=500$	K3 $\eta'=1000$	Ham62 $\eta'=500$
PF00001	0.608	0.569	0.565	0.541	0.516	0.484	0.374	0.346
PF00013	0.909	0.909	0.889	0.889	0.857	0.821	0.679	0.643
PF00014	0.889	0.889	0.625	0.688	0.750	0.708	0.625	0.563
PF00018	0.889	0.889	0.933	0.933	0.909	0.909	0.667	0.667
PF00028	0.944	0.944	0.933	0.900	0.889	0.889	0.802	0.813
PF00059	0.810	0.857	0.771	0.771	0.774	0.774	0.598	0.617
PF00071	0.844	0.875	0.811	0.811	0.763	0.788	0.652	0.646
PF00072	0.810	0.762	0.778	0.778	0.759	0.796	0.685	0.713
PF00075	0.760	0.720	0.738	0.643	0.714	0.619	0.579	0.548
PF00076	0.786	0.786	0.870	0.870	0.857	0.857	0.757	0.743
PF00085	0.800	0.800	0.758	0.727	0.740	0.720	0.650	0.680
PF00089	0.977	0.954	0.847	0.833	0.796	0.815	0.724	0.687
PF00254	0.895	0.895	0.807	0.807	0.851	0.809	0.674	0.632
PF00307	0.714	0.714	0.629	0.571	0.547	0.528	0.449	0.430
PF00486	0.786	0.714	0.708	0.708	0.649	0.622	0.527	0.554
Average	0.828	0.818	0.777	0.765	0.758	0.743	0.629	0.619

Table S5: Positive predictive value of the RLS algorithm for different values of the pseudocounts λ

FAM	Top L/5					Top L/3					Top L/2					Top L				
	$\lambda=0$	$\lambda=20$	$\lambda=44$	$\lambda=200$	$\lambda=1000$	$\lambda=0$	$\lambda=20$	$\lambda=44$	$\lambda=200$	$\lambda=1000$	$\lambda=0$	$\lambda=20$	$\lambda=44$	$\lambda=200$	$\lambda=1000$	$\lambda=0$	$\lambda=20$	$\lambda=44$	$\lambda=200$	$\lambda=1000$
PF00001	0.608	0.608	0.608	0.628	0.647	0.553	0.553	0.565	0.565	0.577	0.523	0.516	0.516	0.492	0.484	0.358	0.366	0.374	0.381	0.374
PF00013	0.818	0.909	0.909	0.909	0.818	0.889	0.889	0.889	0.889	0.889	0.821	0.821	0.857	0.857	0.857	0.661	0.661	0.679	0.661	0.661
PF00014	0.889	0.889	0.889	0.889	0.778	0.688	0.688	0.625	0.625	0.500	0.750	0.750	0.750	0.625	0.458	0.625	0.625	0.625	0.604	0.542
PF00018	0.889	0.889	0.889	0.889	0.889	0.933	0.933	0.933	0.933	0.933	0.818	0.864	0.909	0.864	0.864	0.644	0.667	0.667	0.667	0.644
PF00028	0.944	0.944	0.944	0.889	0.889	0.900	0.900	0.933	0.933	0.933	0.889	0.889	0.889	0.889	0.889	0.813	0.813	0.802	0.802	0.813
PF00059	0.810	0.810	0.810	0.714	0.714	0.800	0.800	0.771	0.771	0.714	0.774	0.774	0.774	0.774	0.736	0.570	0.570	0.598	0.626	0.551
PF00071	0.844	0.844	0.844	0.844	0.813	0.811	0.811	0.811	0.811	0.755	0.763	0.775	0.763	0.763	0.763	0.646	0.646	0.652	0.646	0.634
PF00072	0.810	0.810	0.810	0.810	0.810	0.778	0.778	0.778	0.778	0.778	0.759	0.759	0.759	0.759	0.778	0.685	0.685	0.685	0.694	0.685
PF00075	0.720	0.760	0.760	0.760	0.680	0.691	0.714	0.738	0.738	0.762	0.698	0.714	0.714	0.698	0.651	0.540	0.548	0.579	0.556	0.516
PF00076	0.786	0.786	0.786	0.786	0.786	0.870	0.870	0.870	0.870	0.870	0.857	0.857	0.857	0.857	0.857	0.757	0.757	0.757	0.757	0.729
PF00085	0.800	0.800	0.800	0.800	0.800	0.758	0.758	0.758	0.727	0.727	0.740	0.740	0.740	0.740	0.740	0.640	0.650	0.650	0.650	0.620
PF00089	0.977	0.977	0.977	0.977	0.977	0.847	0.847	0.847	0.861	0.861	0.796	0.806	0.796	0.796	0.787	0.724	0.724	0.724	0.714	0.714
PF00254	0.895	0.895	0.895	0.895	0.842	0.807	0.807	0.807	0.807	0.774	0.830	0.830	0.851	0.851	0.809	0.663	0.663	0.674	0.674	0.621
PF00307	0.714	0.714	0.714	0.667	0.476	0.686	0.657	0.629	0.543	0.429	0.623	0.585	0.547	0.491	0.415	0.439	0.430	0.449	0.430	0.327
PF00486	0.786	0.786	0.786	0.786	0.786	0.708	0.708	0.708	0.750	0.708	0.649	0.649	0.649	0.649	0.622	0.514	0.527	0.527	0.541	0.527
Average	0.819	0.828	0.828	0.816	0.780	0.781	0.781	0.777	0.773	0.747	0.753	0.755	0.758	0.740	0.714	0.619	0.622	0.629	0.627	0.597

Table S6: Positive predictive value for short range (5-11) medium range (12-23) and long range (>23) contacts on top L/5 pairs

FAM	Short range			Medium range			Long range		
	RLS	PSICOV	DCA	RLS	PSICOV	DCA	RLS	PSICOV	DCA
PF00001	0.137	0.196	0.125	0.294	0.255	0.229	0.745	0.510	0.792
PF00013	0.818	0.636	0.909	0.545	0.455	0.545	0.909	0.909	0.909
PF00014	0.667	0.333	0.333	0.889	0.889	0.889	0.778	0.778	0.778
PF00018	0.778	0.778	0.778	1.000	1.000	1.000	0.556	0.333	0.444
PF00028	0.722	0.611	0.647	0.889	0.944	0.941	0.889	0.889	0.882
PF00059	0.810	0.714	0.750	0.619	0.571	0.600	0.762	0.571	0.700
PF00071	0.531	0.469	0.613	0.656	0.656	0.677	0.844	0.719	0.839
PF00072	0.810	0.714	0.857	0.714	0.810	0.810	0.714	0.762	0.810
PF00075	0.320	0.280	0.200	0.400	0.400	0.480	0.800	0.760	0.800
PF00076	0.643	0.786	0.786	0.929	0.929	0.929	0.786	0.714	0.786
PF00085	0.600	0.500	0.632	0.600	0.550	0.632	0.750	0.800	0.684
PF00089	0.581	0.605	0.488	0.791	0.674	0.781	0.837	0.791	0.902
PF00254	0.789	0.737	0.833	0.789	0.684	0.833	0.842	0.737	0.889
PF00307	0.476	0.476	0.350	0.524	0.190	0.600	0.619	0.286	0.650
PF00486	0.786	0.714	0.643	0.571	0.429	0.500	0.571	0.500	0.571
Average	0.631	0.570	0.596	0.681	0.629	0.696	0.760	0.671	0.762